Transport and fate of mercury under different hydrologic regimes in polluted stream in mining area

Yan Lin[1,*], Thorjørn Larssen[1,2], Rolf D. Vogt[1], Xinbin Feng[3], Hua Zhang[3]

1. Department of Chemistry, University of Oslo, POB 1033, 0315 Oslo, Norway. E-mail: yan.lin@kjemi.uio.no
2. Norwegian Institute for Water Research, Gaustadalleen 21, 0349 Oslo, Norway
3. State Key Laboratory of Environmental Geochemistry, Institute of Geochemistry, Chinese Academy of Sciences, Guiyang 550002, China

Abstract

Seepage from Hg mine wastes and calcines contains high concentrations of mercury (Hg). Hg pollution is a major environmental problem in areas with abandoned mercury mines and retorting units. This study evaluates factors, especially the hydrological and sedimentary variables, governing temporal and spatial variation in levels and state of mercury in streams impacted by Hg contaminated runoff. Samples were taken during different flow regimes in the Wanshan Hg mining area in Guizhou Province, China. In its headwaters the sampled streams/rivers pass by several mine wastes and calcines with high concentration of Hg. Seepage causes serious Hg contamination to the downstream area. Concentrations of Hg in water samples showed significant seasonal variations. Periods of higher flow showed high concentrations of total Hg (THg) in water due to more particles being re-suspended and transported. The concentrations of major anions (e.g., Cl^-, F^-, NO_3^- and SO_4^{2-}) were lower during higher flow due to dilution. Due to both sedimentation of particles and dilution from tributaries the concentration of THg decreased from 2100 ng/L to background levels (< 50 ng/L) within 10 km distance downstream. Sedimentation is the main reason for the fast decrease of the concentration, it accounts for 69% and 60% for higher flow and lower flow regimes respectively in the upper part of the stream. Speciation calculation of the dissolved Hg fraction (DHg) (using Visual MINTEQ) showed that $Hg(OH)_2$ associated with dissolved organic matter is the main form of Hg in dissolved phase in surface waters in Wanshan (over 95%).

Key words: mercury; hydrology; temporal variation; fractionation and speciation

DOI: 10.1016/S1001-0742(10)60473-1

Citation: Lin Y, Larssen T, Vogt R D, Feng X B, Zhan H, 2011. Transport and fate of mercury under different hydrologic regimes in polluted stream in mining area. Journal of Environmental Sciences, 23(5): 757–764

Introduction

Hg mining was and still is in some places a serious threat to local environments and human being. Severe Hg contamination in regions with Hg mining and retorting has been documented at many places (Hines et al., 2000; Berzas Nevado et al., 2003; Horvat et al., 2003; Feng and Qiu, 2008). The effect of changes in runoff regimes on Hg levels and fluxes in the contaminated watercourses need to be better understood. Improved understanding of the role of hydrological factors on Hg mobilization and transport is especially important in places where there are large fluctuations in hydrological conditions. This is the case for river systems located in subtropical monsoon areas as they are subject to large fluctuations in precipitation between dry and rainy seasons.

Hg contamination is a serious problem in many places in the world, especially in previous mining areas, such as Almadén in Spain, Idrija in Slovenia and Wanshan

in Guizhou, China. Streams that drain these areas carry large amount of Hg containing particles to the downstream environment. Studies have been conducted on identifying the physical and chemical forms of Hg in natural aquatic system. Hg(II) is found to be most abundant oxidation state of Hg in normal aquatic system (Ullrich et al., 2001). Hg(II) is mainly associated with particles as well as dissolved organic matter (DOM) (Lindqvist et al., 1991).

Re-suspension and transport of particles in streams is known to be high during higher flow (Horvat et al., 2003). During periods of higher flow it is therefore hypothesized that the fluxes of particle bound Hg is greater and the distance the contaminated particles are transported downstream is longer. To conceptually unravel the different mechanisms governing the empirical differences with flow regimes it is necessary to identify the main chemical forms of Hg under different hydrological regimes.

This study focuses on the impacts of different hydrologic conditions on Hg transportation and its fractionation and speciation. The studied area, Wanshan County in east Guizhou Province, lies in the subtropical monsoon

---

* Corresponding author. E-mail: yan.lin@kjemi.uio.no

area of south west China. This area usually experiences a long rainy period in summer caused by tropical air masses from both the Pacific Ocean and Indian Ocean. The winter months are typically cold and dry. Riverflow rises significantly during the rainy season and returns to lower flow during the winter months. Wanshan also lies in the centre of the circum-Pacific mercuriferous belt (Qiu et al., 2006) and has a long history of Hg mining and processing. Between 1949 and early 1990s approximately 126 million tons of calcine from the roasted ore was deposited (Feng and Qiu, 2008). Up to 4.4 g/kg of total Hg (THg) in calcines has been found in Wanshan (Qiu et al., 2005). Although Hg mining and retorting activities have been banned since 2001, the huge historic deposits of Hg contaminated calcines are continuing to leak Hg into the local environment. Several research articles have documented the Hg levels in different environmental media in the Wanshan area. Concentrations of THg in surface water collected at Xiaxi River proximal to calcines were found to be as high as 11 μg/L, while dissolved Hg concentration was as high as 0.66 μg/L (Horvat et al., 2003). Concentration of methyl Hg (MeHg) also showed similar pattern with highest value of 0.77 ng/L (Horvat et al., 2003). Another study showed that water draining calcine piles had a pH of about 11 and dissolved Hg concentrations of up to 1.9 μg/L (Zhang et al., 2004). Water from these streams has been used for irrigation, causing Hg contamination of agricultural soil. Up to 790 mg/kg Hg was found in rice paddy soil in the Wanshan area (Qiu et al., 2005). Recent studies by Zhang et al. (2010a, 2010b) showed that THg concentration was as high as 2.0 μg/L at Xiaxi Stream and MeHg was up to 11 ng/L. Most of these studies focused on documentation of Hg levels, and data from different time of sampling showed quite different results. It is therefore important to address the factors that affect the Hg concentration and transportation. The impact of hydrologic conditions on Hg transformation is the main focus of this study.

1 Materials and methods

1.1 Study area

The watercourse starts with Aozhai and Xiaxi tributaries which merge together at AX01 producing the Dashuixi River that flows north-eastward into Jinjiang River at AX05 (Fig. 1). Both headwater tributaries pass by large calcine tailings at locations that are marked. The calcine is discarded residue after retorting of limestone containing cinnabar. Contaminated water is used for irrigation during the dry season when alternative uncontaminated water sources are not available. River water was collected from 24 locations.

1.2 Sample collection and analysis

Water samples were collected in acid pre-cleaned Teflon bottles. In the laboratory, water sample aliquots were filtered (0.45 μm). Collection, storage, and preservation techniques of samples complied with the Method 1631 of
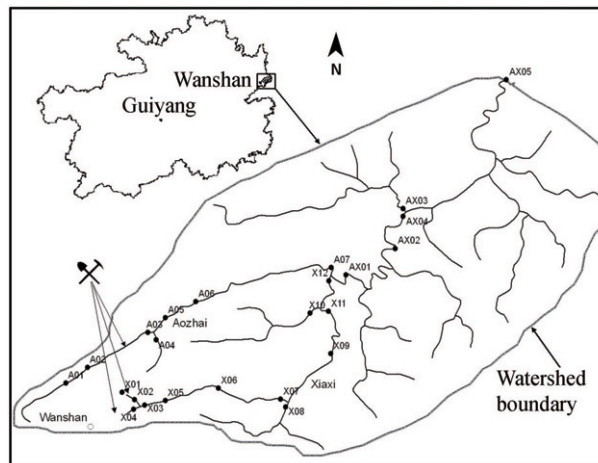

Fig. 1 Map of the Wanshan region with Aozhai and Xiaxi Stream. The sampling sites are marked with station codes and the Hg contaminated tailings are marked with X sign.

US EPA (2002). The river could encounter desiccation and freeze-up in winter months according to our observation, this added the difficulty of collecting duplicate samples. September, 2007 and July, 2008 were therefore chosen to conduct sampling work. Summer is supposed to be the rainy season in Guizhou and September is usually transitional period from rainy to dry period. Precipitation data was also obtained from the nearest meteorological monitoring station (Tongren) to ensure the identification of flow conditions since the river flow is mainly supplied by precipitation. The weekly precipitation before the September sampling was 37 mm while the weekly precipitation before the July sampling was 71 mm (CMA, 2008).

Total and dissolved fraction of inorganic (THg, DHg) and methyl mercury (MeHg) were determined by analysing non-filtered and filtered samples, respectively. The particulate mercury fraction (PHg) was obtained by subtracting the dissolved fraction from the total concentration. Inorganic mercury was determined after up-concentration by dual stage gold amalgamation using Cold Vapour Atomic Fluorescence Spectrophotometer (CVAFS) (PSA Merlin, England) (US EPA, 2002). Water samples for MeHg analysis were distilled and ethylated, before detection by CVAFS (Horvat et al., 1993; Liang et al., 1994, 1996). All samples were determined for THg and MeHg concentrations. Major ions were determined by ion chromatography (ISO, 2007), DOC was determined using a wet-dry combustion method (Bisutti et al., 2004). Water samples of 1.5 L were filtered using 0.45 μm filters and filters were dried to constant weight at 103–105°C. Total suspended solids (TSS) was then determined by weight increase of the filters.

1.3 Quality control/quality assurance

The relative percent difference (RPD) on analyses of Hg on the CVAFS was assessed by analyzing blind duplicates. Furthermore, each sample was analyzed three times on each run to achieve an estimate of standard deviation (RSD). Both RPD and RSD of THg analysis were below 8%. Matrix spikes were used to calculate the percent recovery, which ranged from 92% to 110% for THg

analysis. The limit of detection was 0.1 ng/L for THg in water samples. The RSD of MeHg analysis was less than 8%, and RPD of MeHg analysis was <5.4%. Recoveries on matrix spikes of MeHg in water samples were in the range of 83%–115%. Limit of detection was 0.01 ng/L for MeHg in water samples.

2 Results and discussion

2.1 Total and dissolved concentrations of Hg and MeHg

Concentrations of Hg fractions under different hydrologic regimes are presented in Table 1. The THg concentrations during higher flow ranged between 3.8 and 2100 ng/L, with a geometric average of 67 ng/L ($n = 24$) (Fig. 2). During lower flow regime the maximum THg concentrations reached 1200 ng/L, with a geometric average of 30 ng/L ($n = 24$) (Fig. 2). The concentrations of THg and DHg during higher and lower flow regimes were compared by paired-t-test to check for significant difference. THg concentrations showed significantly higher concentration at higher flow ($p < 0.01$), while DHg concentrations did not show a similar pattern ($p = 0.960$) (Table 1).

The Hg contaminated calcines are located at the headwaters of the streams. Concentrations of most Hg fractions become highly elevated in the stream upon passing by these calcine piles, even though concentration decreases again to the level of 50 ng/L (Type I in Chinese surface water standard) within 10 km downstream from the contamination source (Fig. 3). Type I in Chinese surface water standard applies for water quality of headwaters and natural reserves. Concentrations of DHg also became higher upon passing the tailings (Fig. 4). The maximum THg concentration (2100 ng/L) in Wanshan stream water was significantly lower than that observed at Almadén (20,000 ng/L), but higher than that found at Idrija (320
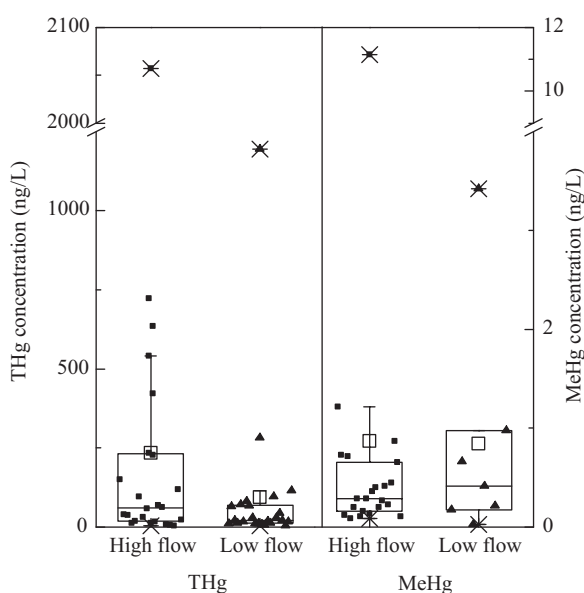
Table 1 Hg concentration of water samples during higher flow (HF) and lower flow (LF)

ID	THg (ng/L)		DHg (ng/L)		MeHg (ng/L)	
	HF	LF	HF	LF	HF	LF
AX05	13	9.3	7.0	8.4	0.14	
AX04	59	13	1.5	8.5	0.29	
AX03	17	6.8	14	5.8	0.36	
AX02	31	10	19	5.3		
AX01	68	18	14	6.9	0.16	
A07	230	28	61	24	0.40	
A06	96	12	18	7.1	0.10	
A05	420	67	30	22		
A04	640	96	300	27	0.20	
A03	540	81	260	13	0.29	
A02	62	29	7.2	13	0.27	
A01	19	16	4.4	14	0.20	0.41
X12	9.3	6.6	7.2	4.5	0.41	
X11	13	13	6.7	8.3	0.088	
X10	5.6	3.7	4.5	2.1	0.23	0.025
X09	39	17	1.9	5.4	0.72	
X08	3.8	3.3	1.1	1.9	0.45	0.21
X07	41	21	6.6	3.7	0.12	3.4
X06	120	65	3.5	7.5	0.87	
X05	230	72	7.5	48	0.73	
X04	150	110	19	33	0.65	0.66
X03	720	280	11	260	1.20	1.0
X02	2100	1200	120	370	11	
X01	24	9.7	13	5.7	0.11	0.17
p-Value	0.006		0.96		0.016*	

THg: total Hg concentration; DHg: dissolved Hg concentration; LF: lower flow (September 2008); HF: higher flow (July, 2009). *p*-Value is paired-*t*-test results to check significant difference of HF and LF values. Blank in MeHg means no samples available. * *p*-Value is only applied for samples with both HF and LF values.
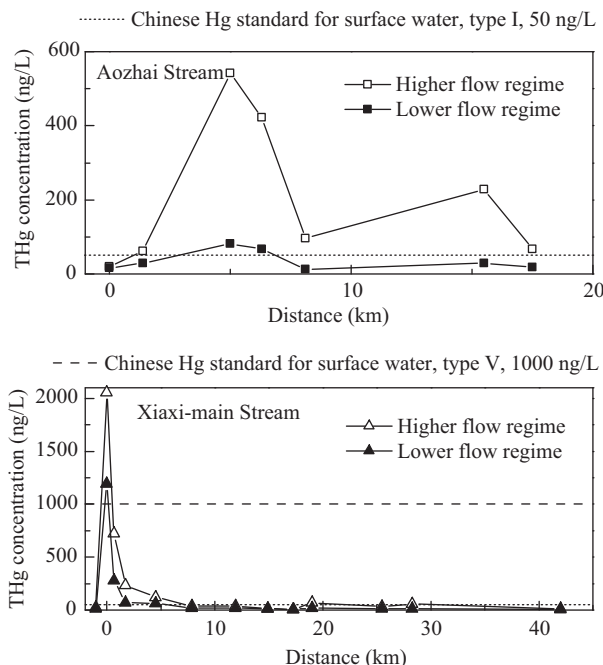

Fig. 3 THg concentrations in Aozhai and Xiaxi in both flow regimes. Note: upper figure shows the concentration of Aozhai Stream from headwater to the merging point with Xiaxi, lower figure shows the concentrations of Xiaxi Stream from headwater to merging point with Aozhai and further downstream until AX05. Type V represents water for agricultural and sightseeing use and type I represents water for headwater and natural reserves based Chinese surface water standard (GB3838-2002).
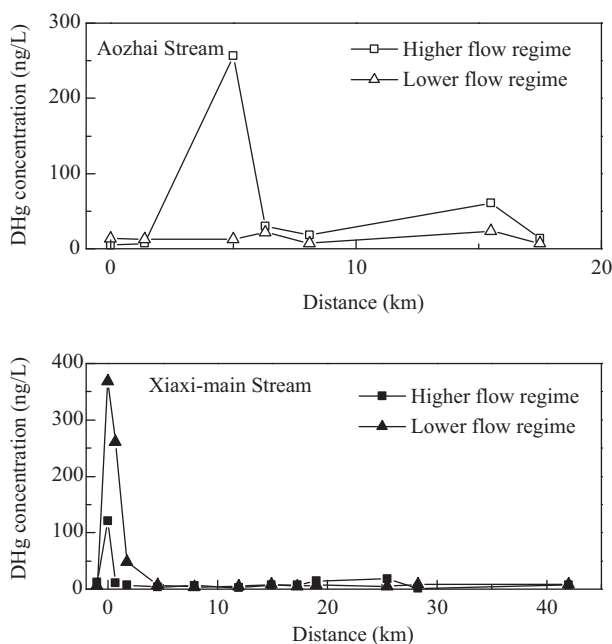

Fig. 2 THg and MeHg concentrations of higher flow and lower flow regimes. Box range 25th–75th percentile of data series, × shows maximum and minimum values of data series, whisker shows 5th–95th percentile of data series.

Fig. 4 DHg concentrations in Aozhai and Xiaxi in both flow regimes. Upper figure shows the concentration of Aozhai Stream from headwater to the merging point with Xiaxi, lower figure shows the concentrations of Xiaxi Stream from headwater to merging point with Aozhai and further downstream until site AX05.

ng/L) (Berzas Nevado et al., 2003; Hines et al., 2000). The maximum THg concentration (2100 ng/L) in this study was also lower than previously reported value (10,580 ng/L) by Horvat et al. (2003) in Wanshan. Since the Hg pollution was widely concerned, pollution reduction measures were taken in recent years. Several sedimentation ponds were built near several important calcine tailings including sites in this study. The sedimentation pond can effectively slow the flow velocity, thus it can reduce a substantial amount of Hg by sedimentation of the Hg contained particles. The results of this study showed THg concentration was indeed decreased compared with the data published by Horvat et al. (2003).

MeHg concentrations constituted less than 5% of THg concentrations in most samples. The highest concentration of MeHg (11 ng/L) was found immediate downstream of the calcines. Concentrations of MeHg reached higher levels during higher flow with values ranging between 0.088 and 11 ng/L, although the geometric average was 0.34 ng/L ($n = 22$) (Fig. 2). During lower flow the maximum MeHg concentration reached 3.4 ng/L, although the geometric average of 0.36 ng/L ($n = 7$) was similar to that of lower flow (Fig. 2). Despite higher maximum concentrations during higher flow no significant difference was found in MeHg concentration between the different flow regimes. Some previous studies have also documented similar results. Zhang et al. (2010b) found water samples contained MeHg concentrations ranging from <0.035 to 11 ng/L (geometric mean 0.43 ng/L) during a drought period and from <0.035 to 3.42 ng/L (geometric mean 0.21 ng/L) during a normal flow period.

2.2 Local water chemistry – major ions, pH and total suspended solids (TSS)

The concentrations of major anions and TSS in the stream water increased sharply upon passing by the calcines and decreased again within short distance at downstream. Due to predominance of carbonaceous bedrock in the region, most of the samples have pH value above 7, especially when Xiaxi flows through calcines which cause rapid increase in pH (up to 11). It is clearly that the water chemistry changes dramatically when sampling sites X02 (pH up to 11) and X04 (pH below 7) merge. This also causes different mechanisms in controlling the partitioning and speciation of Hg in upper and lower parts of the stream.

Data from higher and lower flow regimes were compared by paired-t-test to check for significant differences. Concentrations of the major anions (F$^-$, Cl$^-$, NO$_3$$^-$ and SO$_4$$^{2-}$; Table 2) during lower flow are generally higher than those measured during higher flow. Concentration of TSS was significantly higher during higher flow compared to lower flow. Concentration of TSS is known to increase with increasing water flow due to both soil erosion (from the river banks and the flood plain) and sediment resuspension.

Hg is a highly particle reactive element, which does not show conservative behaviour in aquatic systems (Andren and Harriss, 1975). Results showed that big part of THg exists as PHg in the system giving a strong correlation between THg and TSS (0.92 and 0.67 for higher flow and lower flow regimes, respectively) (Fig. 5). This indicates that THg is highly related to suspended particles, and the transportation and speciation of THg is highly controlled by the behaviour of suspended particles and thus hydrology of the stream. Particle transport is also the main explanation for the rapid decline of THg concentration immediate downstream of the contamination source. Similar results were also confirmed by Zhang (2010a).
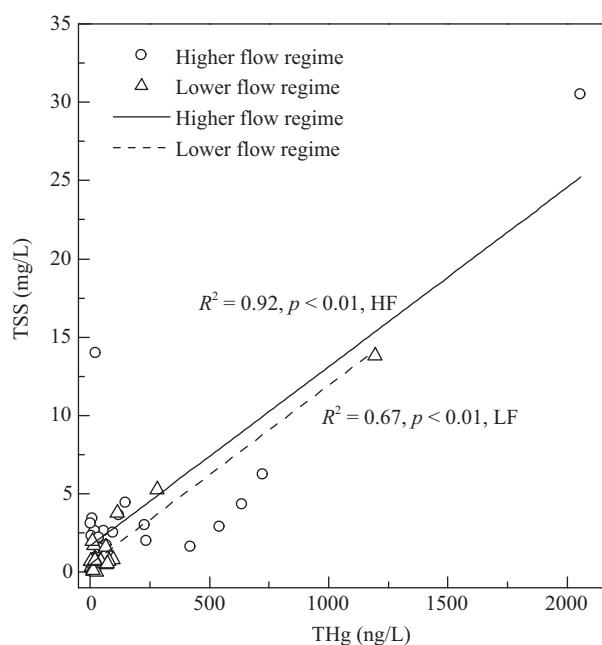

Fig. 5 Correlation between THg and TSS for both flow regimes.

Table 2 Major ions, pH and total suspended solids (TSS) of water samples in different flow regimes

Sampling site	F⁻ (mg/L)		Cl⁻ (mg/L)		NO₃⁻ (mg/L)		SO₄²⁻ (mg/L)		pH		TSS (mg/L)	
	HF	LF	HF	LF	HF	LF	HF	LF	HF	LF	HF	LF
AX05	0.23	2.5	3.1	4.0	7.0	42	52	250	8.3	8.3	2.2	0.21
AX04	0.12	0.11	3.0	4.3	1.1	2.0	18	11	8.1	8.8	2.6	0.068
AX03	0.15	1.9	3.2	4.8	1.4	6.6	26	170	8.4	8.0	2.5	0.31
AX02	0.25	5.1	3.2	4.3	4.5	6.4	32	190	8.2	8.2	2.1	0.68
AX01	0.19	1.9	3.4	5.8	3.6	73	33	540	7.9	8.5	1.7	0.33
A07	0.25	2.2	6.0	10	1.7	96	35	960	8.3	8.5	3.0	0.035
A06	0.2	11	6.5	12	2.8	92	22	1300	7.9	8.2	2.5	0.6
A05	0.29	13	6.6	13	2.4	82	85	1500	8.0	8.1	1.6	0.5
A04	0.23	24	9.6	17	32	93	160	2000	8.1	8.4	4.3	0.8
A03	0.22	23	6.4	16	17	88	120	1900	7.9	8.2	2.9	0.68
A02	0.28	1.9	5.4	4.8	2.4	5.6	39	59	8.1	8.3	1.0	0.6
A01	0.27	0.68	2.2	4.4	2.2	4.7	28	60	8.2	8.4	2.6	0.82
X12	0.17	0.82	2.3	6.2	3.6	59	21	320	7.7	7.7	3.4	0.7
X11	0.16	1.0	2.5	6.8	3.7	77	23	410	7.0	7.1	2.1	0.51
X10	0.19	0.11	5.3	4.0	3.1	2.6	28	14	7.3	7.8	2.3	0.79
X09	0.17	0.59	4.6	8.2	2.0	89	20	420	7.1	7.0	2.2	0.14
X08	0.19	0.17	1.8	4.0	1.9	3.2	30	490	7.2	7.4	3.1	0.67
X07	0.18	3.7	5.0	10	1.2	3.9	78	120	7.0	6.6	1.5	0.76
X06	0.47	4.0	6.5	10	0.89	6.3	30	490	6.9	6.5	3.6	1.7
X05	0.38	4.2	6.7	14	0.89	110	23	1200	6.9	5.4	2.0	1.6
X04	0.46	4.3	10	6.5	0.73	140	17	1700	6.6	5.1	4.4	3.8
X03	0.46	3.8	10	16	1.5	160	28	2200	6.7	5.3	6.2	5.3
X02	0.23	4.4	13	20	7.7	160	54	2500	11	11	31	14
X01	0.21	0.15	1.0	1.4	1.7	2.3	37	58	8.2	8.3	14	2.0
p-Value	0.003		0		0		0		0.002*		0.001	

LF: lower flow (September 2008); HF: higher flow (July, 2009).

p-Value is paired-t-test results to check significant difference of HF and LF values.

* *p*-Value is paired results of pH value bigger than 7.

2.3 Hydrologic impacts on Hg concentration

Suspended solids are, as described above, hypothesized to be an important media for transportation of Hg. Higher flow results in a higher TSS value in aquatic system, and higher TSS will consequently reflect more particulate bound Hg in the water system, thus giving higher PHg concentration.

In addition to Hg, elevated concentrations of chloride is seeping from the gangue and calcine tailings. Cl⁻ can be conceived as a conservative element (Bonzongo et al.,

Fig. 6 Contribution of dilution effect to THg concentration changes.

2006). Cl⁻ concentration can be therefore used to quantify the relative contribution of dilution and sedimentation to the reduction of THg concentration. Figure 6 (Xiaxi-main stream) shows the changes of THg and Cl⁻ concentrations of both flow regimes. The change of Cl⁻ concentration is assumed to be only affected by dilution. The decrease of THg is much faster than the decrease of Cl⁻ concentration for both flow regimes. Three sections of stream without influence of tributaries were selected to reflect the different conditions of upper, middle and lower watercourses. The three sections are X05–X07 (upper), X09–X11 (middle) and AX01–AX04 (lower).

$C_{\mathrm{Hg}i}$ and $C_{\mathrm{Cl}i}$ represent the Hg and Cl⁻ concentration at point i, respectively. $C^{*}_{\mathrm{Hg}j}$ is the assumed THg concentration at point j without sedimentation. The factor that affects concentration value is dilution.

$$C^{*}_{\mathrm{Hg}j} = C_{\mathrm{Hg}i} \times C_{\mathrm{Cl}j} \div C_{\mathrm{Cl}i} \qquad (1)$$

Thus the contribution of dilution (D) to Hg concentration decrease can be estimated as:

$$D = \frac{C_{\mathrm{Hg}i} - C^{*}_{\mathrm{Hg}j}}{C_{\mathrm{Hg}i} - C_{\mathrm{Hg}j}} \qquad (2)$$

The contribution of sedimentation (S) to Hg concentration decrease is:

$$S = 100\% - D \qquad (3)$$

Table 3 shows the results of calculation. It is confirmed that the decrease of THg mainly happens at the upper parts of the stream. The Hg concentration decreased from 2100 to 50 ng/L within 10 km from headwater (Fig. 3).
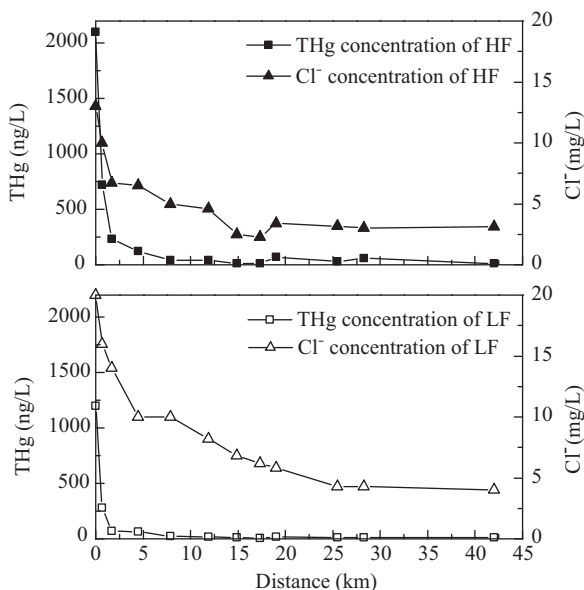
Table 3   Estimate of hydrologic effects on Hg concentration decrease

	Decrease of THg (ng/L)		Contribution of dilution		Contribution of sedimentation	
	HF	LF	HF	LF	HF	LF
Upper (X05–X07)	189	51	31%	40%	69%	60%
Middle (X09–X11)	26	4	68%	73%	32%	27%
Lower (AX01–AX04)	9	5	89%	93%	11%	7%

Sedimentation is the main reason for the fast decrease of the concentration (69% and 60% for higher flow and lower flow regimes respectively) in the upper part of the stream. Studies on THg in stream sediments also showed that THg concentration was as high as 360 mg/kg at upper part of Xiaxi, while at middle and lower part of Xiaxi the THg concentration is just around 10 mg/kg (Lin et al., 2010). This also confirms that majority of Hg is removed from water by sedimentation and deposit as the river sediment. The contribution of dilution becomes more important at the middle part of the stream. At the lower part of stream, THg concentration doesn't change significantly, and dilution completely takes over as the main driver for concentration decrease. The contribution of sedimentation in a higher flow regime is also higher than that of lower flow regime. During higher flow, more particles and larger particles are suspended, more Hg exists as PHg which results in a higher contribution of sedimentation.

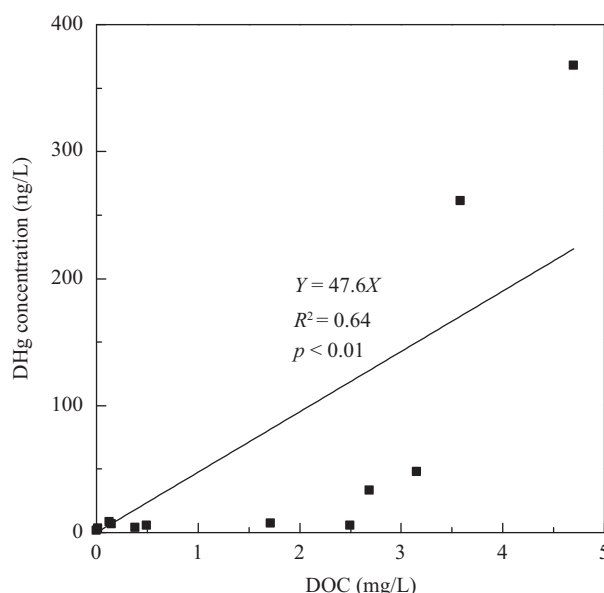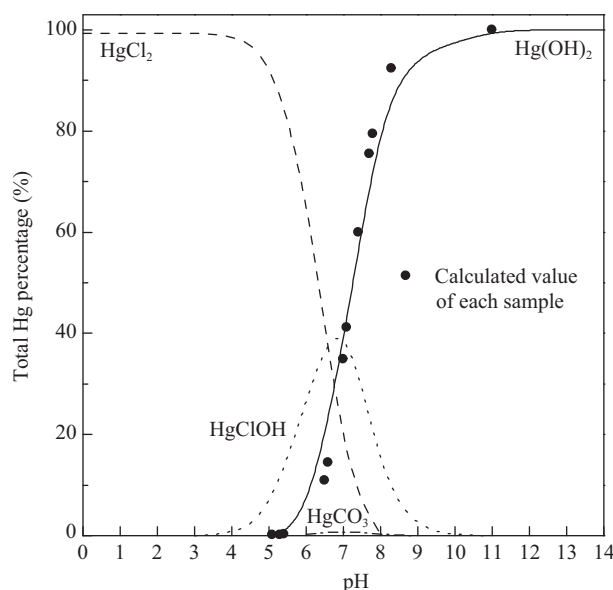## 2.4 Hg species and transformation in both dissolved and solid phases

Water chemistry changes rapidly after it passes through the calcines, it thus also causes dramatic change in factors that control Hg speciation and transformation. X02, X06 and X12 of Xiaxi were subsequently chosen to represent typical conditions of calcine drainage (X02), middle part of stream (X06) and stable status (X12). The behaviour of Hg in the system is mainly controlled by its speciation, which in turn is determined by the chemistry of the water, ligand formation and adsorption processes. Visual MINTEQ was used to simulate the Hg speciation under different water chemistry.

The most important inorganic ligands interacting with Hg^{2+} in these surface waters are OH^-, Cl^- and CO_3^{2-}, while dissolved organic matter (DOM) is the most important organic ligands (Schuster, 1991). The affinity of Hg to these ligands leads to an increased mobility. Xiaxi is chosen to carry out the calculation as it is the most polluted part and also poses wide range of water chemistry. The data including concentrations of Hg, DOC, Cl^- and pH (Tables 1 and 2) were used to simulate the water chemistry of each point to identify the major Hg species. Calcite is set as the infinite solid of the system as limestone is

main bedrock. Dissolved organic carbon (DOC) of Xiaxi in lower flow regime is listed in Table 4. DOM was assumed to be fulvic acid (or humic acid) and Stockholm Humic Model (SHM) was used to calculate the complexation between DOM and Hg^{2+}. Results on both fulvic acid and humic acid showed over 98% of dissolved Hg is complexed with DOM for all samples. Since the majority of dissolved Hg is bound with DOC, DOC and DHg concentration showed good correlation ($R^2 = 0.64$, $p < 0.01$, $n = 12$) (Fig. 7). The Hg that complexed with inorganic ligands is almost

Fig. 7   Correlation between DHg and DOC of water samples.

$$Y = 47.6X$$
$$R^2 = 0.64$$
$$p < 0.01$$

Table 4   DOC of Xiaxi in lower flow regime

Sample site	X01	X02	X03	X04
DOC (mg/L)	2.5	4.7	3.6	2.7
Sample site	X05	X06	X07	X08
DOC (mg/L)	3.2	1.0	1.7	0.01
Sample site	X09	X10	X11	X12
DOC (mg/L)	0.5	0.38	0.13	0.15

Fig. 8   Inorganic Hg species under different pH values.

negligible. Results showed that $Hg(OH)_2$ is the dominant species of inorganic species when pH is above 7, but HgClOH and $HgCl_2$ starts to take over when pH is below 7 (Fig. 8). Powell et al. (2004) has also confirmed similar results which indicates that in a Hg^{2+}-Cl^--CO_3^{2-} system, $Hg(OH)_2$ is dominant species at pH above 7. $Hg(OH)CO_3^-$ is significant at very high HCO_3^- concentration.

Majority of Hg exist as PHg for all samples, as shown in Section 3.1. Iron (Fe) oxides and clays have been found to be the most effective sorbents in neutral to alkali environment (Andersson, 1979; Jackson, 1998). Organic matter can further promote the adsorption of Hg to suspended solids in water (Bilinski et al., 1991; Backstrom et al, 2003; Slowey et al., 2005). The adsorption of Hg to various types of particles including α-quartz, amorphous Fe oxides, α-FeOOH (Geothite) and amorphous silica has been studied (Tiffreau et al., 1995; Bonnissel-Gissinger et al., 1999). Under pH 7–9 around 90% of Hg can be adsorbed by goethite while 50% can be adsorbed by α-quartz and Fe oxides. The existence of natural organic matter can promote the adsorption of Hg on suspended particles (Bilinski et al., 1991; Backstrom et al., 2003), and this makes even more Hg associated with the solid phase. This can explain why most of samples have high concentration of PHg. But at pH 11, no particle can adsorb as much Hg as sample X02. This indicates a different mechanism which controls the partitioning of Hg at site X02. Since X02 is just below the out flow from calcines, the solution is saturated with $CaCO_3$. Blinski et al. (1991) have shown that 96% of Hg can be adsorbed by calcite in natural water and thus precipitate to the streambed. Therefore, the co-precipitation of Hg on calcite is the main explanation of high PHg concentration at very high pH value.

3 Conclusions

This study shows that in the Wanshan area, with slightly alkaline aquatic environment, concentrations of Hg are highly controlled by the prevailing hydrologic conditions. Particulate bound Hg is the main Hg fraction in the system. Significantly elevated THg concentrations were observed during higher flow conditions due to that more suspended solids are re-suspended.

THg concentrations decreased within short distance downstream of the contamination source. Sedimentation of suspended solids is the main mechanism for the initial fast decline in the THg (69% and 60% for higher flow and lower flow regimes respectively), while dilution gradually takes over as the main governing factor after 10 km downstream of the contamination source. Sedimentation is more important during higher flow regime due to more suspended particles. The concentration of major ions also showed clear difference between different flow regimes. Lack of dilution during lower flow period resulted in high solute concentration. THg showed the opposite trend with low concentrations during lower flow due to less particle transport during lower flow velocity.

The use of Visual MINTEQ showed that Hg^{2+} associated with DOM is the main form of Hg (over 98%) in dissolved phase in Wanshan stream water, while Hg adsorbed by both Fe oxyhydroxide dominate the forms of Hg on suspended particulate matter except places with very high pH (pH 11). Co-precipitation of Hg on calcite is the main reason for decline of THg concentration at places where precipitation of calcite was observed.

References

Andersson A, 1979. Mercury in soils. In: The Biogeochemistry of Mercury in the Environment (Nriagu J O, ed.). Elsevier/North Holland Biomedical Press, Amsterdam, New York, Oxford. 79–122.

Andren A, Harriss R, 1975. Observation on the association between mercury and organic matter dissolved in natural waters. *Geochimica et Cosmochimica Acta*, 39(9): 1253–1257.

Backstrom M, Dario M, Karlsson S, Allard B, 2003. Effects of a fulvic acid on the adsorption of mercury and cadmium on goethite. *The Science of Total Environment*, 304(1-3): 257–268.

Berzas N J J, Garcia B L F, Rodriguez M-D R C, 2003. Distribution of mercury in the aquatic environment at Almadén, Spain. *Environmental Pollution*, 122(2): 261–271.

Bilinski H, Kozar S, Plavsic M, Kwokal Z, Branica M, 1991. Trace metal adsorption on inorganic solid phase under estuarine conditions. *Marine Chemistry*, 32(2-4): 225–233.

Bisutti I, Hilke I, Raessler M, 2004. Determination of total organic carbon – an overview of current methods. *Trends in Analytical Chemistry*, 23(10-11): 716–726.

Bonnissel-Gissinger P, Alnot M, Lickes J, Ehrhardt J, Behra P, 1999. Modeling the adsorption of mercury(II) on (hydr)oxides II. α-FeOOH (Geothite) and amorphous silica. *Journal of Colloid and Interface Science*, 215(2): 313–322.

Bonzongo J, Nemer B W, Lyons W B, 2006. Hydrologic controls on water chemistry and mercury biotransformation on a closed river system: the Carson River, Nevada. *Applied Geochemistry*, 21(11): 1999–2009.

CMA (China Meteorological Administration), 2008. China meteorological data daily value. China Meteorological Data Sharing Service System. http://cdc.cma.gov.cn/. Beijing, China.

Feng X, Qiu G, 2008. Mercury pollution in Guizhou, Southwestern China – An overview. *Science of the Total Environment*, 400(1-3): 227–237.

Hines M E, Horvat M, Faganeli J, Bonzongo J C, Barkay T, Major E B et al., 2000. Mercury biogeochemistry in the Idrija Stream, Slovenia, from above the mine into the Gulf of Trieste. *Environmental Research*, 83(2): 129–139.

Horvat M, Bloom N S, Liang L, 1993. A comparison of distillation with other current isolation methods for the determination of methyl mercury compounds in low level environmental samples, Part 2: Water. *Analytica Chimica Acta*, 282(1): 153–168.

Horvat M, Nolde N, Fajon V, Jereb V, Logar M, Lojen S et al., 2003. Total mercury, methylmercury and selenium in

mercury polluted areas in the province Guizhou, China. *Science of the Total Environment*, 304(1-3): 231–256.

ISO (International Organization for Standardization), 2007. ISO 10304-1:2007: Water quality – Determination of dissolved anions by liquid chromatography of ions – Part 1: Determination of bromide, chloride, fluoride, nitrate, nitrite, phosphate and sulfate. Geneva, Switzerland.

Jackson T A, 1998. Mercury in aquatic ecosystems. In: Metal Metabolism in Aquatic Environments (Langston W J, Bebianno M J, eds.). Chapman and Hall Publishers, London. 77–157.

Liang L, Horvat M, Bloom N S, 1994. An improved speciation method for mercury by GC/CVAFS after aqueous phase ethylation and room temperature precollection. *Talanta*, 41(3): 371–379.

Liang L, Horvat M, Cernichiari E, Gelein B, Balogh S, 1996. Simple solvent extraction technique for elimination of matrix interferences in the determination of methylmercury in environmental and biological samples by ethylation-gas chromatography-cold vapor atomic fluorescence spectrometry. *Talanta*, 43(11): 1883–1888.

Lin Y, Larssen T, Vogt R D, Feng X, 2010. Identification of fractions of mercury in water, soil and sediment from a typical Hg mining area in Wanshan, Guizhou province, China. *Applied Geochemistry*, 25(1): 60–68.

Lindqvist O, Johansson K, Aastrup M, Andersson A et al., 1991. Mercury in the Swedish environment – recent research on causes, consequences and corrective methods. *Water, Air and Soil Pollution*, 55(1-2): 7–17.

Powell K J, Brown P L, Byrne R H, Gajda T, Hefter G, Sjöberg S et al., 2004. Chemical speciation of Hg(II) with environmental inorganic ligands. *Australian Journal of Chemistry*, 57: 993–1000.

Qiu G L, Feng X B, Wang S F, Shang L H, 2005. Mercury and methylmercury in riparian soil, sediments, mine-waste calcines, and moss from abandoned Hg mines in east Guizhou province, southwestern China. *Applied Geochemistry*, 20(3): 627–638.

Qiu G L, Feng X B, Wang S F, Shang L H, 2006. Environmental contamination of mercury from Hg-mining areas in Wuchuan northeastern Guizhou, China. *Environmental Pollution*, 142(3): 549–558.

Schuster E, 1991. The behavior of mercury in the soil with special emphasis on complexation and adsorption processes-a review of the literature. *Water, Air and Soil Pollution*, 56(1): 667–680.

Slowey A, Johnson S, Rytuba J, Brown G, 2005. Role of organic acids in promoting colloidal transport of mercury from mine tailings. *Environmental Science & Technology*, 39(20): 7869–7874.

Tiffreau C, Lutzenkirchen J, Behra P, 1995. Modeling the adsorption of Hg(II) on (hydr)oxides I. Amorphous iron oxide and α-quartz. *Journal of Colloid and Interface Science*, 172(1): 82–93.

Ullrich S M, Tanton T W, Abdrashitova S A, 2001. Mercury in the aquatic environment: A review of factors affecting methylation. *Critical Reviews in Environmental Science and Technology*, 31(3): 241–293.

US EPA (United States Environmental Protection Agency), 2002. Method 1631, Revision E: Mercury in water by oxidation, purge and trap, and cold vapor atomic fluorescence spectrometry. United States Environmental Protection Agency, Office of Water 4303, EPA-821-R-99-005, Washington DC, USA.

Zhang H, Feng X B, Larssen T, Shang L H, Vogt R D, Rothenberg S E, 2010a. Fractionation, distribution and transport of mercury in rivers and tributaries around Wanshan Hg mining district, Guizhou Province, Southwestern China: Part 1 – Total mercury. *Applied Geochemistry*. DOI: 10.1016/j.apgeochem.2010.01.006

Zhang H, Feng X B, Larssen T, Shang L H, Vogt R D, Lin Y, 2010b. Fractionation, distribution and transport of mercury in rivers and tributaries around Wanshan Hg mining district, Guizhou Province, Southwestern China: Part 2 – Methylmercury. *Applied Geochemistry*. DOI: 10.1016/j.apgeochem.2010.01.005